

PAPER • OPEN ACCESS

## Simulation of natural convection in a solar collector

To cite this article: Jura Jumaev *et al* 2023 *J. Phys.: Conf. Ser.* **2573** 012024

View the [article online](#) for updates and enhancements.

A promotional banner for the 244th ECS Meeting. The left side has a teal background with the ECS logo and text: "244th ECS Meeting", "Gothenburg, Sweden • Oct 8 – 12, 2023", "Register and join us in advancing science!", and "Learn More & Register Now!". The right side features a graphic with silhouettes of people, a city skyline, and a network of nodes and lines, all set against a bright sun background.

**ECS** 244th ECS Meeting  
Gothenburg, Sweden • Oct 8 – 12, 2023  
Register and join us in  
advancing science!  
Learn More & Register Now!

# Simulation of natural convection in a solar collector

**Jura Jumaev\*, Jobir Kodirov and Shavkat Mirzaev**

Bukhara State University, Bukhara, Uzbekistan

\*E-mail: j.jumaev@buxdu.uz

**Abstract.** The process of natural convection in a flat solar collector, which was designed by the authors, was mathematically modeled using experimental data. Stones were used as storage means. The inclined collector is expressed as a two-dimensional plate for modeling. The initial and boundary conditions were formulated. It was assumed that the flow in this region is laminar. To simulate the flow of natural air convection, a system of non-stationary partial differential equations was chosen based on the laws of conservation of mass, momentum and energy in the Boussinesq approximation. The equations were solved in a dimensionless form using the finite difference method and an explicit scheme. The picture of the temperature fields and the appearance of convection was obtained on the basis of experimental temperature data in the inlet and outlet zones of the collector, as well as on the surface of the heat accumulator during the day. To evaluate the effectiveness of the resulting model an average approximation error (approximation) of 7.7% was established. The results obtained in specific values of the Grashof and Prandtl numbers are presented in the form of graphs.

## 1. Introduction

In solar dryers with natural air circulation, there is a convection mode, a comprehensive study of such processes is a very urgent problem of hydromechanics and heat transfer, since they are often found in many practical problems related to the efficient use of renewable energy sources, the relevance of which is reflected in numerous scientific papers related to them.

In the works of the authors [1], the details of a mathematical model for collectors with perforated adsorbers are presented using heat transfer expressions for their elements, to identify empirical relationships, and also to evaluate various heat transfer coefficients. The equations used predict thermal performance well over a wide range of collector designs and operating conditions. The results of the mathematical model were analyzed to predict the effects of the main performance parameters of the collector systems in the supply air temperature range (35-55) °C.

The study of the authors [2] is focused on the analysis of the temperature profile, heat transfer characteristics and thermal efficiency of a flat plate solar collector (FPSAC) at various mass airflows. Also, with the help of multivariate analysis of the study, relationships were established among several other variables of thermal characteristics.

Experiments were carried out in an unloaded mode and in the open air under the conditions of natural and forced air convection in the collector of a solar dryer.

An analysis of the principal parametric components made it possible to visualize the association among solar intensity, temperature in various reservoir elements, heat transfer coefficients, thermal efficiency and time of day. The results show that the useful heat gain, the heat transfer coefficient of the air and the thermal efficiency of the collector do not strongly depend on the intensity of solar radiation.



In [3], a numerical analysis of the study of the convective flow of a viscous incompressible fluid over an inclined semi-infinite plate was carried out, taking into account the dependence of viscosity and thermal diffusivity on temperature. Equations are identified with the corresponding boundary conditions, which are converted to a dimensionless form using the corresponding dimensionless quantities. In the numerical solution, the authors used the Crank-Nicolson scheme as the most efficient and unconditionally stable implicit finite difference method.

Numerical results were obtained for various values of viscosity, thermal conductivity, absorber inclination angle, Grashof and Prandtl criteria. The results of studying the change in speed, temperature, shear stress and Nusselt number are presented graphically. For the reliability of the results, a comparison was made with the results available in the literature.

In the article of the authors [4], the process of the emergence of dynamic and temperature boundary layers near a vertically located rod, which is a source of heat, is modeled. A stationary system of differential equations in partial derivatives is formulated in the boundary layer approximation and also considering the medium to be compressible. The problem with boundary conditions is solved numerically using an implicit scheme using the sweep and iteration method. Velocity and temperature profiles are found for various values of the Prandtl number and boundary conditions. It has been established that the results of the study can be used for the process of convection near heat sources.

From the analysis of the results of the above literature, it can be concluded that the processes found in flat-plate collectors with natural air convection need further research, for example, solar collectors using different materials for storage means, mathematical modeling in close contact with the results of experimental studies.

## 2. Experiments and materials

For an experimental study of convection, we designed a flat solar collector, which is connected and located below the drying cabinet. The angle of inclination of the outer surface of the bottom of the collector is set from  $38^\circ$  to  $45^\circ$  in relation to the horizon in order to concentrate and transfer the maximum amount of solar heat to the drying cabinet. Trays are installed in the drying cabinet, in which mesh trays with dried fruits are placed (figure 1).

The purpose of this article is to mathematically model the process of generating warm air with natural convection based on experimental data in this flat plate solar collector [5].

The inclined flat solar air collector consists of a glass cover 1, a body of the collector chamber 2 thermally insulated from the environment, a heat accumulator (pebbles) 3, a window for air entry 4 into the collector and a window for the exit of heated air 5 from the collector (figure 1).

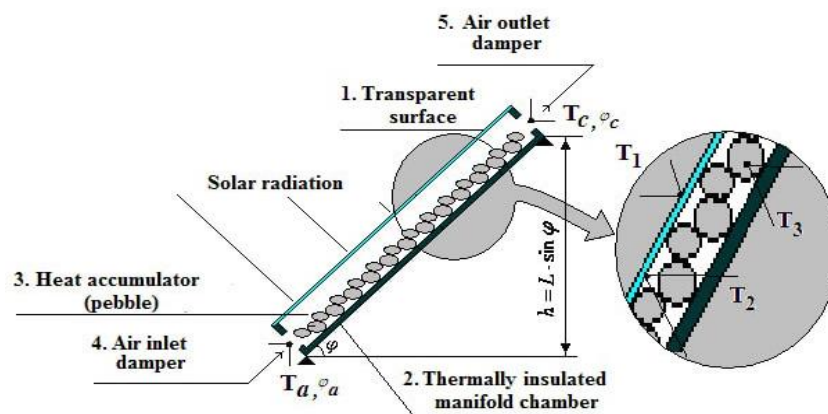


**Figure 1.** View of an inclined flat solar air collector.

The principle of operation of the collector (physical model of the collector): from the glass cover 1, solar radiation enters the bulk air and the surface of the heat accumulator (pebble) 3, which are located

in the collector chamber 2, and heat them. Accumulator 3 accumulates heat during solar irradiation and at the same time heats the air. Thus, the air is heated both from solar radiation and from the heat accumulator at the same time. By increasing the temperature of the air inside the collector chamber, the density decreases. By changing the density, an air flow of warm air is created in the direction of decreasing density (or increasing temperature). In this case, if air enters the collector chamber from the inlet damper, which is located in the lower part of the collector, then the flow of heated air moves towards the upper damper.

### 3. Methods

For mathematical modeling of the process of air convection, let's mentally cut out a vertical plane from this collector in the form of figure 2 and consider a two-dimensional area.

Let us reduce the problem to the study of air convection between two parallel rods [6, 7].

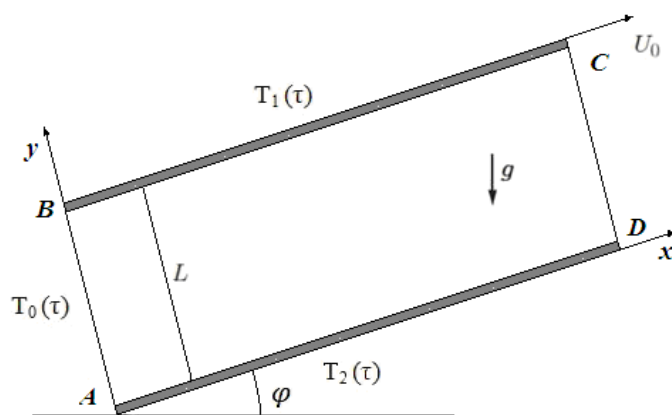


**Figure 2.** Collector scheme and coordinate system.

When forming the initial conditions, we assume that the movement of the air flow has not yet begun inside the collector and its temperature is taken from the experimental data.

The basic equations for a non-stationary flow of natural air convection using the law of conservation of mass, momentum, energy in the Boussinesq approximation can be written as [8,9]:

$$\begin{cases} \frac{\partial(u)}{\partial x} + \frac{\partial(\vartheta)}{\partial x} = 0 \\ \frac{\partial u}{\partial t} + u \frac{\partial u}{\partial x} + \vartheta \frac{\partial u}{\partial y} = -\frac{1}{\rho} \frac{\partial P}{\partial x} + \mu \frac{\partial^2 u}{\partial y^2} - \beta g(T - T_0) \cdot \sin\varphi \\ \frac{\partial T}{\partial t} + u \frac{\partial T}{\partial x} + \vartheta \frac{\partial T}{\partial y} = \alpha \frac{\partial^2 T}{\partial y^2} \end{cases} \quad (1)$$

In equation (2.27)  $u$ ,  $\vartheta$ -are the longitudinal and transverse components of the velocity,  $T$  -is the temperature,  $\rho$ -is the density,  $P$ -is the pressure, which in the study is assumed to be constant and equals the atmospheric pressure,  $\mu$  -is the dynamic viscosity,  $x, y$ -are the coordinates,  $g$  -is the acceleration free fall,  $\beta$  -is the volumetric coefficient of thermal expansion (for air at 30<sup>0</sup> rhu barb  $3.3 \cdot 10^{-3}(1/K)$ ),  $\alpha$  – coefficient of thermal conductivity of the medium.

Statement of boundary conditions. To set the boundary conditions, we turn to figure 2. In the coordinate system, a heat source-rods is located along the axis. The rod has a constant temperature. When the temperature of the rod is higher than the ambient air temperature, dynamic and thermal boundary layers arise near the rod due to air convection, which expand as the air moves upward.

The main parameter for the boundary conditions is the temperature at the boundaries of the collector elements. From the experimentally created collector for hot days, 6 days were selected, ambient temperature data were taken, at the inlet and outlet of the collector air, directly under the glass, at the surface of the heat accumulator.

**Table 1.** Initial and boundary conditions

Border conditions	$u$	$\vartheta$	$T$
AB	$\frac{\partial u}{\partial y} = 0$	$\vartheta = 0$	$T = T_0(\tau)$
BC	$u = 0$	$\vartheta = 0$	$T = T_0(\tau)$
CD	$\frac{\partial u}{\partial y} = 0$	$\frac{\partial u}{\partial y} = 0$	$\frac{\partial T}{\partial y} = 0$
DA	$u = 0$	$\vartheta = 0$	$T = T_0(\tau)$

To solve the differential equation (1), data are needed at each nodal point (in measurement points). To do this, you can build a regression equation using the least squares method.

In this article, using experimental data, a regression equation was compiled in the form of a polynomial. Averaged experimental data (temperatures) under the glass ( $T_1$ ) and in the surface of the heat accumulator ( $T_2$ ), as well as the temperature at the collector inlet ( $T_0$ ) (table 2).

**Table 2.** Averaged experimental data under the glass and the heat accumulator is as follows.

Time	10-00	1-00	12-00	13-00	14-00	15-00	16-00	17-00	18-00	19-00
$T_1$	37.2	43.2	45.5	47.1	50.2	50.7	48.9	45.6	41.3	38.7
$T_2$	46.2	54.2	60.3	63.5	65.6	63.8	60.5	58.4	45.9	40.2
$T_0$	31.3	32.7	35.1	37.4	36.6	37.4	37.4	36.2	36.9	35.9

Using the data of this table, the lines of regression equations are determined in the form:

$$T_1(\tau) = -0.59\tau^2 + 18.786\tau - 89.36.$$

$$T_2(\tau) = -0.826\tau^2 + 24.76\tau - 114.137.$$

$$T_o(\tau) = -0.221\tau^2 + 6.349\tau + 7.281.$$

The system of equations (1) in dimensionless form can be written as:

$$\begin{cases} \frac{\partial(u)}{\partial x} + \frac{\partial(\vartheta)}{\partial x} = 0 \\ \frac{\partial u}{\partial t} + u \frac{\partial u}{\partial x} + \vartheta \frac{\partial u}{\partial y} = \frac{1}{\sqrt{Gr}} \frac{\partial^2 u}{\partial y^2} + \theta \cdot \sin\varphi, \\ \frac{\partial \theta}{\partial t} + u \frac{\partial \theta}{\partial x} + \vartheta \frac{\partial \theta}{\partial y} = \frac{1}{Pr \cdot \sqrt{Gr}} \frac{\partial^2 \theta}{\partial y^2} \end{cases} \quad (2)$$

Here  $Gr = \frac{g \cdot \beta \cdot \Delta T \cdot L^3}{\nu_m^2}$  - Grashof number,  $\Delta T = T_h - T_0$ , where  $T_h$  - maximum collector temperature,  $T_0$ - minimum collector temperature,  $\theta = \frac{T-T_0}{T_h-T_0}$

The equations in such a dimensionless form were solved using the finite difference method and an explicit scheme [10,11].

#### 4. Results and discussion

Figure 3 shows the calculated data on the temperature distribution along the radial temperature distribution at the beginning and at the end of the reservoir, calculated from the data by 10:00 am. One can see the effect of temperature near the surface of the heat accumulator in the vertical direction of the collector.

These influences will be felt at the end of the day, for example, figure 4 shows the temperature distributions obtained by 6 pm (6 pm). It can be seen from the figure that, according to the boundary conditions, the temperature is already low, but due to the accumulation of heat inside the collector, its influence is still noticeable.

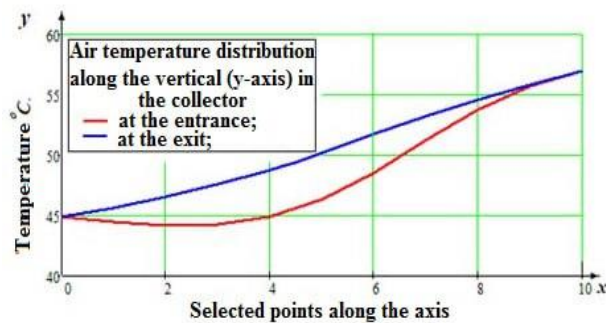


**Figure 3.** Calculated data of temperature distribution at the beginning and at the end of the collector at the beginning of the day.

The influence of convection on occurrences in the vertically directed velocity can be observed in figure 5 and figure 6. Figure 5 shows the velocity distributions at the beginning and end of the collector at the beginning of the day. Due to the influence of the temperature factor, the speed at the end of the collector becomes twice as high as at the beginning of the collector. The velocity maximum is shifted to the side where the temperature prevails. But the influence of the lifting force is also traced, because the maximum speed is shifted to the left from the place where the temperature maximum is located.

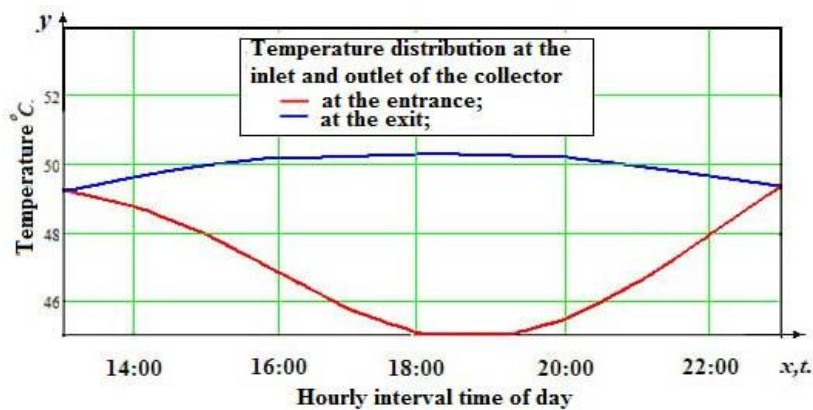


**Figure 4.** Temperature distribution at the beginning and at the end of the collector at the end of the day.



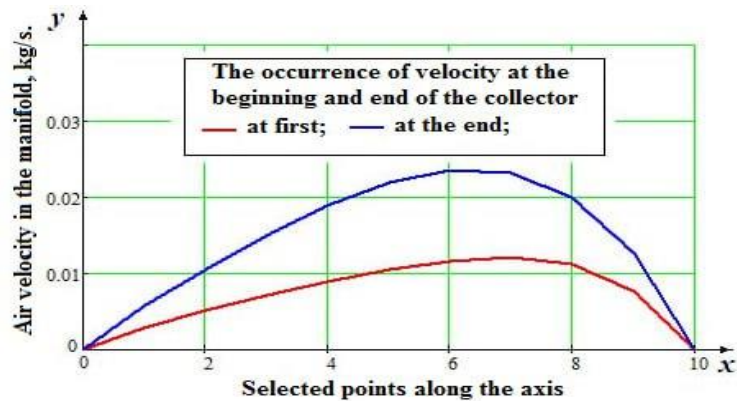


**Figure 5.** The occurrence of velocity at the beginning and end of the reservoir, according to data obtained at the beginning of the day.

The lift effect is still strong when the temperature becomes even higher in the collector. For example, figure 6 shows the vertical velocity data at the beginning and at the end of the collector by 15:00. It can be seen that the maximum speed is shifted towards the middle, its value is twice as high as at the beginning of the day. From this we can conclude that the maximum heat transfer from the collector occurs due to convection by the second half of the day.

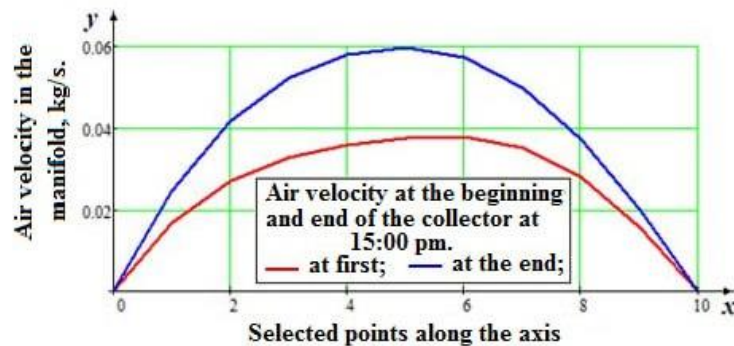


**Figure 6.** The occurrence of velocity at the beginning and end of the reservoir, according to data obtained at 15-00 pm.

A three-dimensional image of the longitudinal velocity distribution in the reservoir is shown in figure 7. The data for this figure is taken in the middle of the day, where the appearance and uniform increase in velocity along the length of the reservoir can be seen. You can see the velocity distribution lines at the beginning of the collector, the increase in values as you move to the top of the collector.

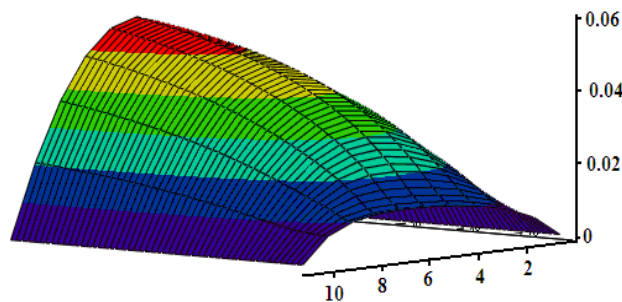


**Figure 7.** Longitudinal speed distribution on the collector in the middle of the day.

## 5. Conclusion

The dependence of air temperatures at the inlet and outlet of the collector, as well as in the surface of the heat accumulator on the measurement time, was established, experimental and calculated data were compared, that is, a clear picture of the relationship between variables was established and compared based on multivariate analysis methods. To evaluate the effectiveness of the resulting model, an average approximation error of 7.7% was revealed. The price of the model also increases the level of confidence in the production of hot (warm) air with natural circulation in flat plate solar collectors.

## References

- [1] Augustus Leon A and Kumar S 2007 *Solar Energy* **81** 62-75
- [2] Poonam Rani and Tripathy P P 2020 *Solar Energy* **211** 464-77
- [3] Palani G, Kirubavati J D and Kwan Y K 2014 *Thermophysics and Aeromechanics* **21** 65-85
- [4] Jumayev J, Shirinov Z and Kuldashv H 2019 Computer simulation of the convection process near a vertically located source *International conference on information Science and Communications Technologiyes (ICISCT)* pp 635-8
- [5] Mirzaev Sh, Kodirov J and Khamraev S I 2022 *IOP Conf. Series: Earth and Environmental Science* **1070** 012021
- [6] Terekhov V I and Ekaid A L 2012 Laminar free convection between vertical parallel plates with different temperatures *Thermophysics and Aeromechanics* **19(4)**
- [7] Maundu Nicholas Musembi *et al.* 2017 *American Journal of Energy Research* **5(1)** 12-22
- [8] Gebhart B, Jaluriya J, Mahajan R L and Sammakia B 1991 *Free-convective flows, heat and mass transfer* (M.: Mir)
- [9] Jumaev M, Sharipov M, Rizoqulov M and Ergasheva N 2021 *Journal of Physics: Conference Series* **1889** 022073
- [10] Anderson D, Tannehill J and Pletcher R 1990 *Computational fluid mechanics and heat transfer* **2** (M: Mir)
- [11] Jumaev J and Opokina N A 2021 *Solving mathematical problems in the mathematical software packages Maxima and MathCAD* (Kazan: KFU)